DEVELOPMENT OF A DYNAMICALLY TUNED GYROSCOPE – DTG

Fernando de Castro Junqueira
Escola Politécnica da Universidade de São Paulo - EPUSP
fcjunq@usp.br

Ettore Apolônio de Barros
Escola Politécnica da Universidade de São Paulo - EPUSP
eabarros@usp.br

Abstract. *This work describes the design and the implementation of a DTG gyroscope. The general aspects about its development, the main difficulties involved, as well as some performance results are discussed. Through the study of a tuned gyroscope operation theory and its errors model, one can analyze the DTG fundamentals and evaluate its main error sources. An analysis of the constructive requirements, the machining methods and materials employed in the DTG implementation are presented. Afterwords, it is done a description of the main characterization tests, that are carried out in order to establish the tuning conditions and to calculate the error model compensation coefficients. Results of these tests are discussed, and the estimation of the random drift, which is the main parameter that qualifies the gyroscope, is presented. The DTG prototype was able to provide a reasonable performance, which satisfies the requisites of several applications.*

Keywords. *Inertial Sensor, Gyroscope, DTG.*

1. Introduction

Inertial sensors (gyroscopes and accelerometers) are an important component for a number of civil and military applications. Robotics, autonomous vehicles, airplanes, ships, satellites and offshore platforms are some examples of civil use. One also can mention the stabilization of weapons and radars, missiles and torpedoes as military examples. These applications make us to realize the importance for many countries of having their own development of inertial technology.

Particularly, the gyroscopes usually involve high cost manufacturing processes, sophisticated technology and expertise, so that the necessary performance on vehicle navigation or device positioning can be achieved. A dynamic tuned gyroscope, the so-called DTG, is one of the options nowadays that can provide the required performance for many applications at a reasonable price. They demand considerable less investment in materials, machinery, processes and man power when compared to the other usual sensors such as the floated or ring-laser gyroscopes. DTG is a two degree-of-freedom sensor that measures angular rates and can achieve precisions better than 0.01 ^{o}/h, in a full-scale range of 200 ^{o}/s.

This work discusses the development of a DTG, emphasizing the aspects of fabrication and performance evaluation. Fundamentals and mathematical modeling of a single-gimbaled DTG are briefly introduced at next section. Section 3 presents the main errors that may corrupt the sensor output, and are unavoidable for the inherent characteristics of the DTG. Construction of a DTG is discussed on section 4 based on details of a prototype that was implemented. Typical performance tests of a DTG are analyzed in section 5, where also some experimental results using the prototype are shown.

2. Dynamic Model

The DTG operation principle is based on an inertia rotor suspended by a universal joint with flexure pivots (figure 1). The flexure spring stiffness is independent of spin rate. However, the dynamic inertia (from the gyroscopic reaction effect) from the gimbal provides negative spring stiffness proportional to the square of the spin speed (Howe and Savet, 1964; Lawrence, 1998). Therefore, at a particular speed, called the tuning speed, the two moments cancel each other, freeing the rotor from torque, a necessary condition for an ideal gyroscope (figure 2).

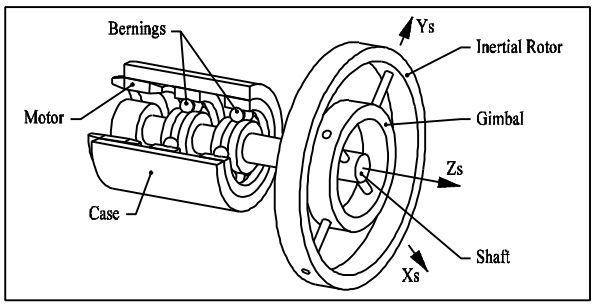

Figure 2.1 – DTG Configuration

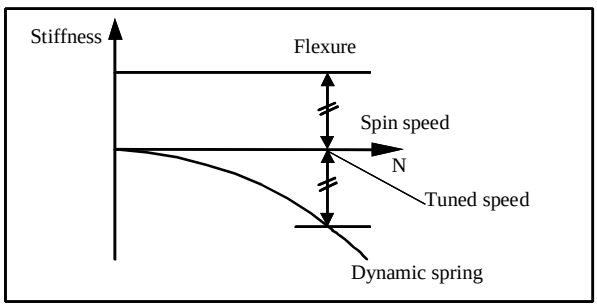

Figure 2.2 –The Tuning Speed

2.1 Mathematical Modeling

A complete model was derived by Craig (1972) for a DTG composed by an arbitrary number of gimbals. Based on his work a simplified model is presented, as in (IEEE, 1989).

The flexible joint is responsible for transmitting spring torques ($k \cdot q_{xc}$, $k \cdot q_{yc}$) and gyroscopic reactions ($N^2 \cdot J \cdot q_{xc}$, $N^2 \cdot J \cdot q_{yc}$), that cancel each other at the tuning speed. Other inertia moments transmitted by the joint are oscillating at a frequency, which is the double of the spin speed.

A drag moment T_d, between case and rotor, is proportional to the spin speed N. It acts on the motor axis direction (z_s), and has components ($-Td \cdot q_y$) and ($Td \cdot q_x$) on the x_r and y_r respectively. There are also moments from the viscous damping, proportional to the relative angular speeds between case and rotor, $Dr \cdot \dot{q}_{xc}$ e $Dr \cdot \dot{q}_{yc}$, acting on directions x_c e y_c respectively.

The torque coils apply moments, MC_x, MC_y, that are used in the control loops on the case axes x_c e y_c, respectively.

Considering the case motions as the inputs, the rotor dynamic equations based on the case fixed coordinates, for axi-symmetric gimbal and rotor, are as follows:

$$\ddot{q}_{xc} I + \dot{q}_{xc}(D + D_r) + q_{xc}(k - N^2 J) + \dot{q}_{yc} N(C + A_g) + q_{yc}(T_d + ND) = -\ddot{f}_x I - \dot{f}_y N(C + A_g - J) + MC_x - q_x \cos 2Nt - q_y \operatorname{sen} 2Nt \quad (2.1)$$

$$\ddot{q}_{yc} I + \dot{q}_{yc}(D + D_r) + q_{yc}(k - N^2 J) + \dot{q}_{xc} N(-C - A_g) - q_{xc}(T_D + DN) = -\ddot{f}_y I + \dot{f}_x N(C + A_g - J) + MC_y - q_x \operatorname{sen} 2Nt + q_y \cos 2N\mathrm{t} \quad (2.2)$$

where,

C, C_g are the rotor, and gimbal z axis moments of inertia, respectively;

A, A_g are the rotor, and gimbal transverse axis moments of inertia, respectively;

$\dot{q}_{xc}$, $\dot{q}_{yc}$ are the rotor angular velocity along the case "x" and "y" axes;

$\dot{f}_{xc}$, $\dot{f}_{yc}$ are the absolute angular velocities of the gyroscope case, resolved along the case-fixed coordinate set.

$$I = \frac{1}{2}(2A + A_g)$$

$$J = \frac{1}{2}(2A_g - C_g)$$

$$q_x = \ddot{q}_{xc}\Delta I + q_{xc} N^2 \Delta J + \dot{q}_{yc} N \Delta I + q_{yc} + \ddot{f}_x \Delta I - \dot{f}_y N(\Delta I + \Delta I_S)$$

$$q_y = \ddot{q}_{yc}\Delta I - q_{yc} N^2 \Delta J - \dot{q}_{xc} 2N \Delta I + \ddot{f}_y \Delta I - \dot{f}_x N(\Delta I + \Delta I_S)$$

$$\Delta I = \frac{1}{2} A_g$$

$$\Delta I_S = \frac{1}{2}(C_g - A_g)$$

$$\Delta J = \frac{1}{2}(C_g - 2A_g)$$

The ideal behavior of a DTG comes from assuming the gimbal inertias are much less than the rotor inertias (so, the terms q_x and q_y can be neglected). After considering very low damping torques, the rotor equations in the open loop ($MC_x = MC_y = 0$), at the tuning speed ($N = N_o = \sqrt{k/J}$) are reduced to:

$$\ddot{q}_{xc} I + \dot{q}_{yc} NC = -\ddot{f}_x I - \dot{f}_y NC \quad (2.3)$$

$$\ddot{q}_{yc} I - \dot{q}_{xc} NC = -\ddot{f}_y I + \dot{f}_x NC \quad (2.4)$$

Thus, the rotor is free from external moments. For the same initial conditions, case and rotor have opposite displacements in the case-fixed coordinates set:

$$q_{xc}(t) = -f_x(t) \tag{2.5}$$

$$q_{yc}(t) = -f_y(t) \tag{2.6}$$

In closed-loop operation, the rotor inclinations are measured by a pair of sensors and controlled by the torque coils in order to track the case movements. The torque coils interact to a radial magnetic field generated by annular magnets placed on rotor. By measuring the control currents, proportional to the case angular rates, one can measure the vehicle angular rates.

3. Error Model

The design and the manufacturing of a high performance gyroscopic sensor, must take into account several characteristics that are not so important in a normal sensor. So the knowledge of the phenomena that can cause reading disturbances is a need condition to avoid, minimize or compensate them.

The torque free rotor is the basis of the sensor, so every event that causes torque into the rotor, should be compensated by the close loop currents, causing a false case movement interpretation. This way, the DTG errors analysis, can be done by researching the torque causes.

As derivate by Craig, (1972b), the constant bias can be shown in eq. 3.1 and 3.2. These errors are mainly caused by angular offsets between rotor and case ($f_x(0)$, $f_y(0)$), the mistuning (dN), the damping time constant (t) and the Figure of Merit (F_m) that is a relationship between the rotor and the gimbal inertias. Large values for F_m or t, and lower values for offsets and the mistuning will minimize these errors. The figure of merit must be maximized during the design step, while the damping should be minimized, by carefully manufacturing the hinge. Fortunately, these errors can be compensating by using the error model, as wheel as other errors.

$$\dot{q}_x(t) = \frac{f_x(0)}{t} + f_y(0) \cdot \frac{dN}{F_m} \tag{3.1}$$

$$\dot{q}_y(t) = \frac{f_y(0)}{t} - f_x(0) \cdot \frac{dN}{F_m} \tag{3.2}$$

Many other error sources are known and well described by Craig (1972c), and Joos (1977) that can be mentioned as follows:

Direct “g” sensitivity: Caused by the axial different position between rotor center of mass, and the hinge center of rotation, that cause a torque when the gyro experiments an linear acceleration in “x” or “y” axis.

Quadrature “g” sensitivity: Can be caused by a defective hinge, and causes he same effect as the direct, but in the orthogonal direction.

Anisoelastic drifts whose values depend on the simultaneous presence of an axial and a lateral acceleration. Careful design can minimize this type of drift.

Synchronous vibration rectification errors: The DTG is sensitive to vibrations at spin speed harmonics. 1st harmonic in an axial vibration couples with the rotor radial unbalance. 2nd harmonic angular vibration, about “x” or “y” direction interacts with the gimbal angular momentum and rectifies to a fixed drift.

Uncompensable drifts are random in nature and principally caused by inevitable ball bearings run out. Thermal gradients are also responsible for magnetic and aerodynamic changings. These drifts are described by two quantities: Day-to-day drift, often referred to as repeatability, and random drift. These drifts cannot be easily compensated because they are only predictable on a probabilistic basis. The quality of a DTG is normally assessed by the values of its dynamic range, its day-to-day drift, and its long-term random drift.

4. Construction Details

The DTG manufacturing is a quite demanding task. It is a small electro-mechanical device whose parts should de made and assembled at very small tolerances.

In this section, a DTG prototype implementation is presented. Case fixed parts and rotating parts are described together their materials and their manufacturing technologies. Special attention is given to the elastic suspension and to the balancing process.

4.1 Main Components of a DTG

Figure 4.1 shows the internal components. The case is made of medium strength steel, supporting all the internal components in a low and constant pressure environment. It should have stable dimensions and works as a magnetic shield.

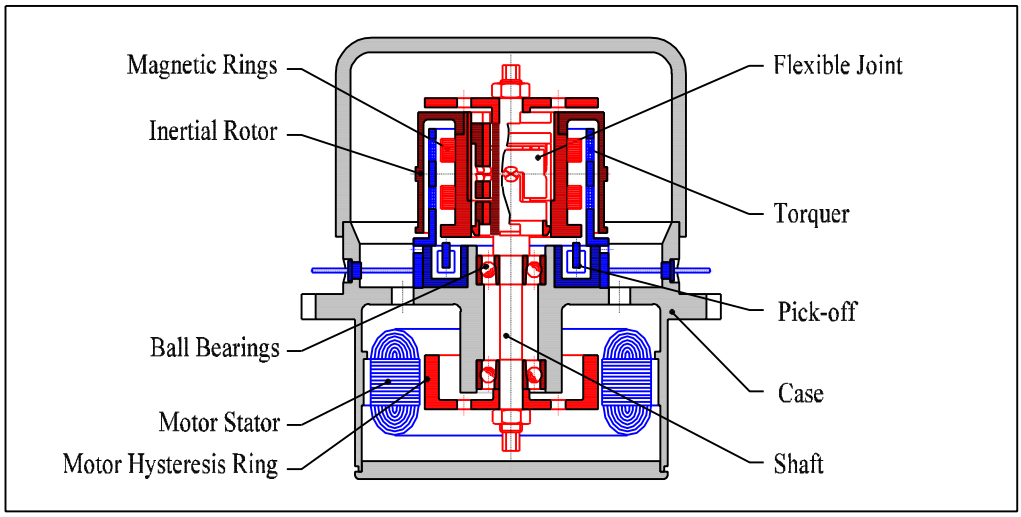

Figure 4.1 - Transverse Cut of a DTG

4.1.1 Case Fixed Components

The fixed parts include the motor, pickoffs, torquer coils and the ball bearings. Due to their reduced sizes those parts are difficult to be manipulated and assembled.

The torquer coils are made of enameled copper wires. It has a curve shape (fig. 4.2) and it is bonded with great care at the case in order to define with high precision the gyroscope output axis.

The pickoff cores are made in 0.1 mm thick Fe-Si blades cut by wire electro-discharge machine. After mounting procedure, the reference surfaces are grinded to enhance the final positioning precision. The pickoff set is composed by four variable reluctance transformers, excited at 50 kHz frequency, and placed at 90 degrees from each other (fig. 4.3). The signals of the opposite transformers are subtracted generating the corresponding angular displacement information.

A synchronous hysteresis motor, driven by a three-phase inverter is responsible for keeping the gyroscope shaft at constant spin speed.

The motor stator is composed by 0.1 mm sheets, while the rotor is a Maraging steel massive ring. This material is submitted to a special heat treatment, which is responsible for the rotor desired magnetic properties.

Machining and the assembling the case fixed parts are tasks that require special skills, but they can be classified as high precision. The fig. 4.4 shows these items as well as the shaft and the electric connections.

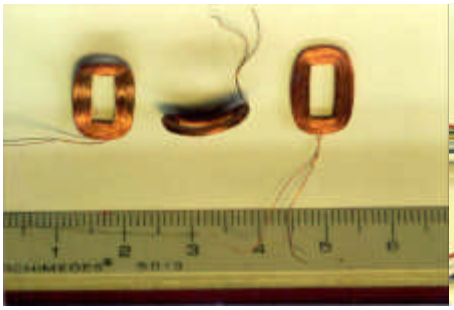

Figure. 4.2 - Torquer Curved Coils

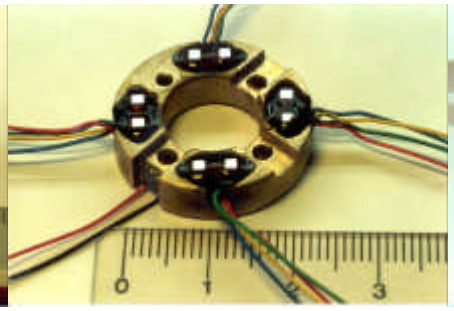

Figure 4.3 - Pickoff Set

Figure 4.4 - Case Fixed Assembling

4.1.2 Rotating Components

The major manufacturing difficulty lies on the rotating parts machining. They require high precision qualities that can only be achieved through special machines as well as very well minded processes.

The shaft (fig. 4.5) is made in medium strength steel. Typical dimensions are 3 mm diameter and 50 mm length, which should show a straightness and circularity precision about 1 or 2µm. For this prototype, 7µm precision was achieved.

The hubs, rotors and rings (fig 4.7) present the same needs in precision, so the final rotating assembling precision remains below 20 μm.

Figure 4.5 – Shaft

Figure 4.6 – Magnetic Ring

Figure 4.7 – Hubs, Ring and Shaft

The inertial rotor, composed by two parts (the two largest parts in fig 4.7) also requires the same precision quality. They are made in pure iron (Fe ARMCO), due to its magnetic properties, avoiding saturations and hysteresis, so better linearity of the scale factor is achieved.

The ball bearings are the most sensitive item of the gyro. They must have high precision quality (ABEC 7). The lubricant oil, which comes from the factory in an ideal quantity, must have low vapor pressure to not evaporate when the case would be evacuate. The initial pre load at assembling procedure to avoid clearances must be done with care not to over load and make damages in the bearings, increasing friction and reducing the life. The pre load can be adjusted by measuring the desacceleration time. The environment to manipulate the bearings should be in a clean area to eliminate dust and reduce the running noise, and also the life.

In special there are two parts deserving attention: The magnetic rings and the flexible joint.

The magnetic rings (fig. 4.6) are responsible for the magnetic field, in which the torquer coils are placed to interact with, leading to the control torques. These rings must have radial magnetic direction. As there are no continuous rings with such property, the solution is dividing the rings in angular sectors in such a way to approximate a radial field. The sectors are made by wire electro-discharge machine from high-energy Nd-Fe-B bricks. After assembled the sectors in a ring, the final dimensions are achieved by using a circular grinding machine with diamond. The final step is the magnetization that is made by placing the rings, one by one, between two equal coils. When an intense pulse current passes by the coils a strong radial magnetic field is generated in that place where the ring lies.

The most difficult item to be done is the flexible joint (fig 4.8a,b). As one can see in Haberland (1978) and Mansour and Lacchini (1993), the usual solution is based in a monolithic construction that satisfies the precision articulation concept, avoiding friction, mechanical gaps and hysteresis on the movements. Besides, this solution permits the coincidence of the centers of rotation (x and y) and the gimbal and the inertial rotor mass centers. The recommended material is high strength steel with low internal strains, to resist the acceleration loads and to minimize deformations after machining. The construction starts from two concentric high precision tubes, where the blades (fig 4.8b) are cut with wire electro-discharge machine. This process is very critical because the thickness of the blades are about 60 μm, (fig 4.9), and can only be achieved with high precision machine that works with 0.05 mm diameter wire. After this step, the two tubes are disassembled and reassembled at 180 degrees from the initial position. The two borders must be welded or bonded and then the final cuts can be done, also in a wire electro-discharge machine, splitting the set in three parts linked only by the blades. The ends will be mounted, one to the shaft and other to the inertial rotor, while the central part is called gimbal.

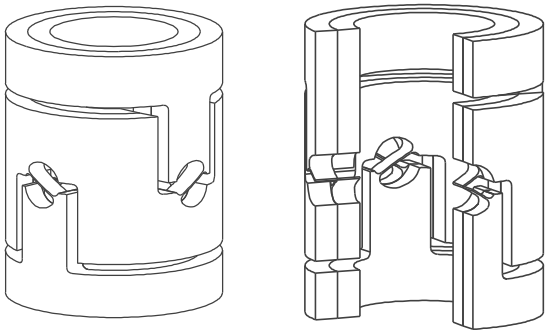

(a) (b)

Figure 4.8 – The Flexible Joint

Figure 4.9 – The Flexible Joint Blades

During the assembling procedure, special attention must be paid to the balancing. The ordinary radial balancing, static and dynamic, was made in a German “Schenk” machine equipped with a laser system to pick off mass while the rotor is running. Another important procedure is the axial balancing, when the axial rotor center of mass is make to coincide to the flexible joint center of rotation. This procedure is executed, with the rotor stopped, by measuring the rotor tilt tendency, when a low frequency lateral vibration is applied to the case.

5. Tests

All the gyroscope tests must be preceded by stabilization procedures to warrant the ideal stable conditions that take long time to be achieved. The most important factor to be controlled is the gyro temperature. Beyond dimensional changes, the temperature causes a variation on the magnetic field with direct influence on the scale factor. The room temperature is also important to be controlled once the electronic apparatus can suffer changes with temperature causing changes on the torquer current readings. A stable table without vibrations is also an important condition to the tests. As needed equipments one can mention precision multimeters and a special inertial system test table, which is a table able to impose angular positions and rates with precision, so various inputs to the inertial systems can be simulated.

5.1 Errors Model

Because of the imperfections, the gyro outputs are strongly influenced by base movements, especially by linear accelerations. Fortunately these influences can be compensated if well known. The equations 5.1 and 5.2 represent a well-accepted error model for DTG.

$$K_{fx} \cdot i_x = b_x + m_x \cdot a_x + qd_x \cdot a_y + u_x \cdot a_z + n_x \cdot a_x \cdot a_z + v_x \cdot a_y \cdot a_z + w_x + w_y \cdot a - w_z \cdot g_y \quad (5.1)$$

$$K_{fy} \cdot i_y = b_y + qd_y \cdot a_x + m_y \cdot a_y + u_y \cdot a_z + v_y \cdot a_x \cdot a_z + n_y \cdot a_y \cdot a_z - w_x \cdot b + w_y + w_z \cdot g_x \quad (5.2)$$

, where,

K_{fx}, K_{fy}	are the scale Factors;
i_x, i_y	are the output currents;
w_x, w_y, w_z	are the input rates;
b_x, b_y	are the constant drift, bias;
m_x, m_y	are the direct ‘g’ sensitive drift on the case-fixed x , and y axes.;
qd_x, qd_y	are the quadrature ‘g’ sensitive drifts;
u_x, u_y	are the axial ‘g’ sensitivite drifts;
n_x, n_y	are the direct aniso-elastic drifts;
v_x, v_y	are the quadrature aniso-elastic drift;
a_x, a_y, a_z	are the case linear accelerations;
a, b, g_x, g_y	are the misalignment angles.

5.2 Tuned Speed Determination

The tuned speed is the one where the gimbal dynamic spring cancels the flexible joint spring, or one can write: $k - N^2 \cdot J = 0$. In this case the speed assumes the value: $N_o = \sqrt{K/J}$. If the gyro is operated in a range of spin speed, and a offset angular position is imposed, there is a linear correspondence between the torque currents and the spin speed, as can be seem below.

$$MC_x = q_{xc}(0) \cdot \frac{2 \cdot k \cdot dN}{N_o} \quad (5.3)$$

Where: $q_c(0)$ is the offset, and
dN is the deviation from the tuned speed.

As can be seen, the linear coefficient depends on the offset value. The tuned speed is given by the crossing of the experimental lines, each one for each choose offset that should cross on the tuned speed once $dN = 0$. The experimental results can be seem in fig.5.1, below, that shows two experiments, one for x and other for y axis. Both figures show the tuned speed about 170 Hz, but there is a small difference between the two values, and a medium value must be taken.

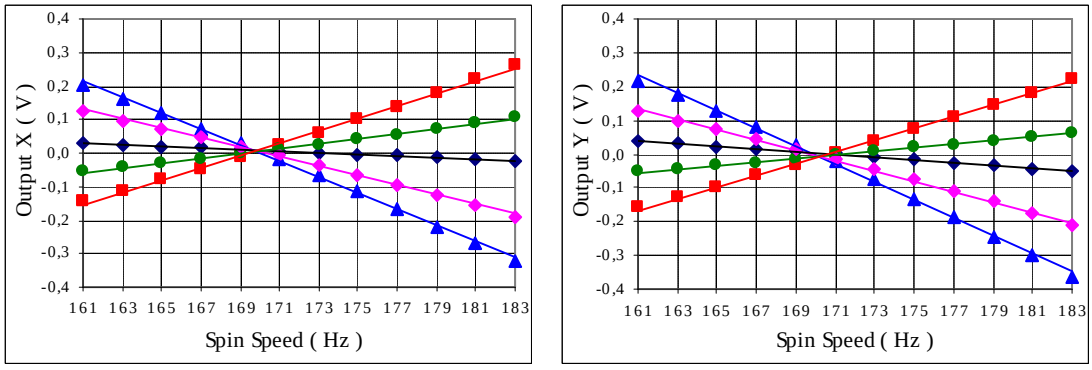

(a) (b)

Figure 5.1 – Experimental results for tuned speed determination

5.3 Determination of the Scale Factor and Internal Misalignments

In a rate table, the gyro is put to work with several constant inputs and the output currents are recorded. This way the linear relationship between input and output are considered the scale factor. As the axis are not perfect, if the both output are recorded the main error angles can be determined. This test is also useful to determine the scale factors linearity and the histeresis.

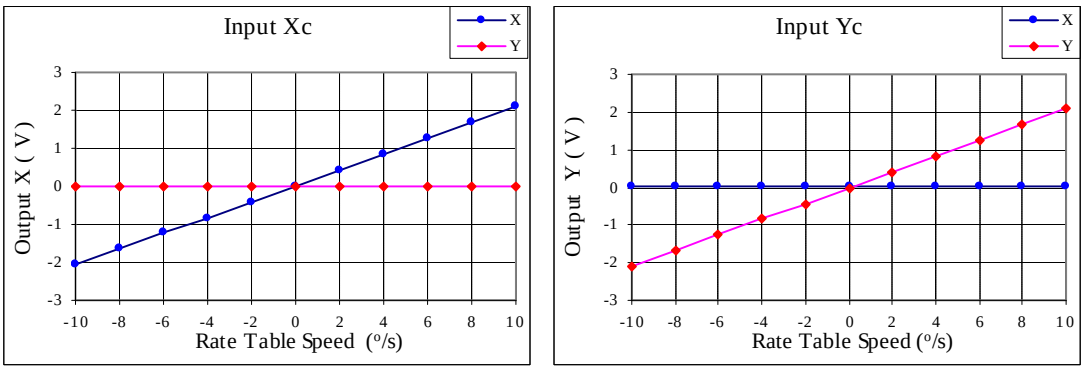

(a) (b)

Figure 5.2 – Determination of the Scale Factors and the Misalignments.

The numeric results are given:

The Scale Factors

K_{fx} = 1656,6 °/h/mA

K_{fy} = 1649,9 °/h/mA

The Misalignments Angles

a = -0,225 degrees

b = -0,026 degrees

Where the non orthogonality angle can be calculated: $b - a$ = 0.200 degrees

5.4 The Multi-Position Test

This test is done to determine the error model coefficients shown in equations 5.1 and 5.2. By placing the gyro in many different positions in relation to the local vertical and north direction, one can simulate several inputs conditions. According to the IEEE-813-1988, the DTG is placed four times with the spin axis in vertical position and four times, in horizontal position. In addition four other positions, 45° in relation to the vertical was done to stimulate acceleration in axial and lateral directions simultaneously in order to determine the anisoelasticity coefficients. With the results, on can make an equation system, whose solution are the drift coefficient values. In fig. 5.3a the results are shown for the 12 positions for both x and y outputs. The calculated expected outputs, considering the error model equation with the calculated coefficient are also shown and fit well to the experimental results. The fig. 5.3b shows the errors between the results and the expected outputs.

The numeric results are given:

b_x =	-289,9 °/h	b_y =	-127,5 °/h
m_x =	-108,4 °/h/g	qd_y =	16,84 °/h/g
qd_x =	-13,72 °/h/g	m_y =	-108,4 °/h/g
u_x =	9,31 °/h/g	u_y =	-18,30 °/h/g
n_x =	-5,76 °/h/g^2	v_y =	0,497 °/h/g^2
v_x =	-5,89 °/h/g^2	n_y =	-0,0623 °/h/g^2

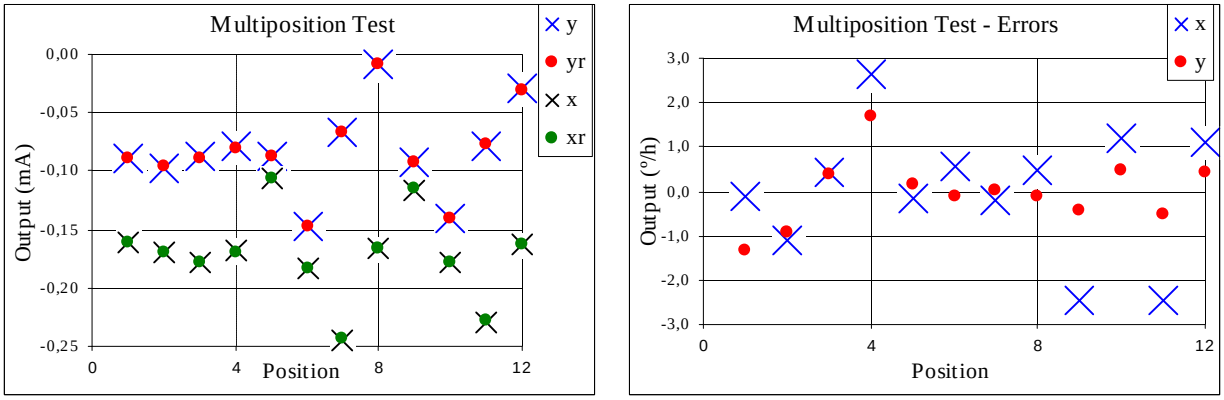

(a) (b)

Figure 5.3 – Multiposition Test Results

5.5 Tumbling Test

In order to verify the coefficients in a different database a tumbling test was performed. This time the DTG spin axis is aligned with the Earth spin axis, 12 positions in North direction and 12 to South. The fig. 5.4(a) shows the results and the expected output, while the fig. 5.4(b) shows the errors, where the maximum error is about 6 °/h.

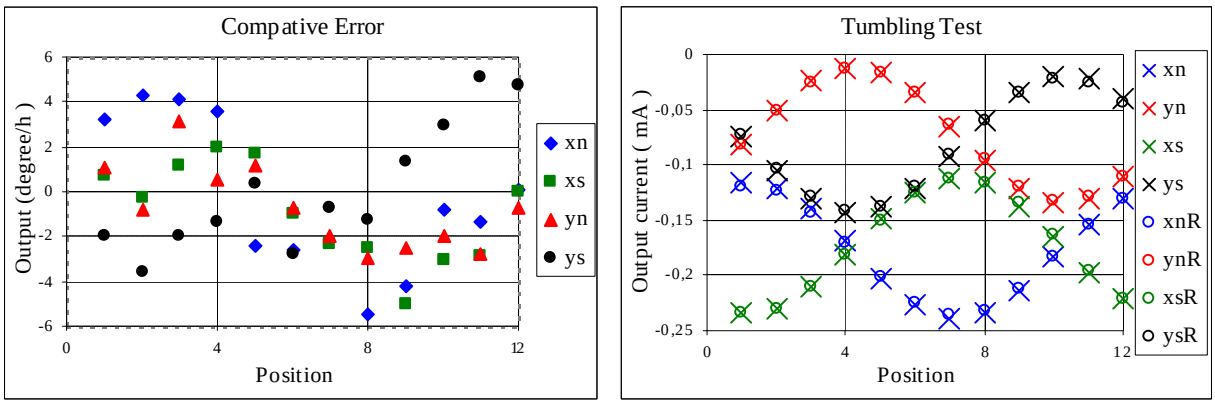

(a) (b)

Figure 5.4 – Tumbling Test Results

5.7 The Random Drift

This test determines the gyro drift that cannot be compensated by an error model, so its results are often used as the main quality parameter. In a fixed position, during two hours, the output signals are recorded at each 30 seconds interval. One mean value is calculated for each 5-minute period. After the full period 12 points are recorded and the standard deviation is the desired result, as can be seen below.

s_x = 0,39 °/h
s_y = 0,49 °/h

6. Conclusions

Experimental validation tests using a DTG prototype confirmed the dynamic tuning effect. The tests also showed reasonable values for linearity and the random bias. The gyroscope time constant is still too low to be considered as a high performance gyroscope parameter. However, a number of applications such as those in the offshore field or satellite launching can probably take advantage of such level of performance. Future developments should include improvement on machining and manufacturing processes for the gyroscope mechanical parts. It is also extremely necessary a constant improvement on the sensor electronics, in order to assure a better accuracy.

7. References

Craig, R. J. G. **Theory of Operation of an Elastically Supported, Tuned Gyroscope**, IEEE Trans. on Aerospace and Electronic Systems, pp. 280-288. vol AES-8, No 3, 1972a.

Craig, R. J. G**. Theory of Errors of a Multigimbal, Elastically Supported, Tuned Gyroscope**, IEEE Trans. on Aerospace and Electronic Systems, pp. 289-297. vol AES-8, No 3, 1972b.

Craig, R. J. G. **Dynamically Tuned Gyros in Strapdown Systems**. AGARD Conference on Inertial Navigation Computers and Systems. Firenze, Italy. pp. 12-1 to 12-17. 1972c.

Haberland, 1978. **Technical Advances through a Novel Gyro Hinge Design**. DGCON Symposium ueber Kreiseltech. Duesseldorf. Germany. Sept. 1978.

Howe, E. W., Savet, P. H. **The Dynamically Tuned Free Rotor Gyro**. Control Engineering. pp. 67-72. June. 1964.

IEEE – Std 813-1988. **Specification Format Guide and Test Procedure for Two-Degree-of Freedom, Dynamically Tuned Gyros**. IEEE, 1989, New York. USA.

Joos, D. K. Comparison of Typical Gyro Errors for Strapdown Applications. DGCON Symposium Gyro Technology, Stuttgart, Germany, 1977.

Karnick, H. **Experience based upon Experimental Dry Tunned Gyros**. DGON Symposium Gyro Technology, Stuttgart, Germany, 1979.

Lawrence, A. **Modern Inertial Navigation: Navigation Guidance, and Control**. Second Edition. Springer. New York. 1998. (Mechanical Engineering Series).

Mansour, W. M., Lacchini, C. **Two-Axis Dry Tuned-Rotor Gyroscope Design and Technology**. Journal of Guidance, Control and Dynamics. Vol 16, No 3, Maio-Junho 1993.